Acta Cryst E CRYSTALLOGRAPHIC COMMUNICATIONS

ISSN 2056-9890

Crystal structure and Hirshfeld surface analysis of 4-{2,2-dichloro-1-[(*E*)-(4-chlorophenyl)diazenyl]-ethenyl}-*N*,*N*-dimethylaniline

Zeliha Atioğlu,[a] Mehmet Akkurt,[b] Namiq Q. Shikhaliyev,[c] Sevinc H. Mukhtarova,[c] Gulnar T. Suleymanova[c] and Flavien A. A. Toze[d]*

[a]İlke Education and Health Foundation, Cappadocia University, Cappadocia Vocational College, The Medical Imaging Techniques Program, 50420 Mustafapaşa, Ürgüp, Nevşehir, Turkey, [b]Department of Physics, Faculty of Sciences, Erciyes University, 38039 Kayseri, Turkey, [c]Organic Chemistry Department, Baku State University, Z. Khalilov str. 23, AZ 1148 Baku, Azerbaijan, and [d]Department of Chemistry, Faculty of Sciences, University of Douala, PO Box 24157, Douala, Republic of , Cameroon. *Correspondence e-mail: toflavien@yahoo.fr

Received 14 April 2020
Accepted 4 June 2020

Edited by M. Weil, Vienna University of Technology, Austria

Keywords: crystal structure; non-covalent interactions; azo dye; Hirshfeld surface analysis.

CCDC reference: 2007970

Supporting information: this article has supporting information at journals.iucr.org/e

The title compound, $C_{16}H_{14}Cl_3N_3$, comprises three molecules of similar shape in the asymmetric unit. The crystal cohesion is ensured by intermolecular C—H···N and C—H···Cl hydrogen bonds in addition to C—Cl···π interactions. Hirshfeld surface analysis and two-dimensional fingerprint plots reveal that Cl···H/H···Cl (33.6%), H···H (27.9%) and C···H/H···C (17.6%) are the most important contributors towards the crystal packing.

1. Chemical context

Non-covalent interactions, such as hydrogen bonds, halogen–halogen or chalcogen–chalcogen bonds, van der Waals interactions or π–π stacking, π···cation and π···anion interactions, *etc*. are much weaker than covalent bonds. Nevertheless, they can control the reactivity of molecules, the crystal packing, tautomerization and other properties (Asadov *et al.*, 2016; Mahmudov *et al.*, 2019). For example, such kinds of weak interactions can create interesting supramolecular networks in coordination compounds, involving monomeric, oligomeric or polymeric subunits, which affects their catalytic activity (Afkhami *et al.*, 2017; Gurbanov *et al.*, 2018).

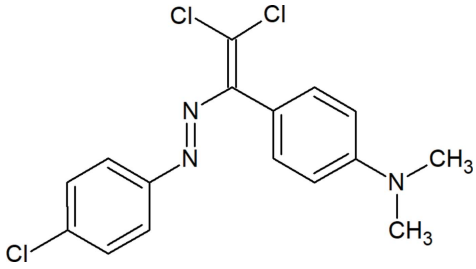

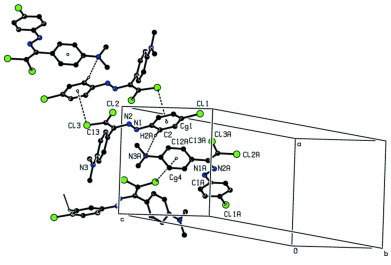

In a previous study we have attached resonance-assisted hydrogen-bonded synthons or chlorine atoms to dye molecules, which leads to intermolecular weak interactions for the resulting products with interesting analytical and solvatochromic properties (Maharramov *et al.*, 2018; Mahmudov & Pombeiro, 2016). In a continuation of our work in this direction, we now have synthesized a new azo dye, 4-{2,2-dichloro-1-[(*E*)-(4-chlorophenyl)diazenyl]ethenyl}-*N*,*N*-dimethylaniline, which features C—H···N, C—H···π and C—Cl···Cl types of weak intermolecular interactions.

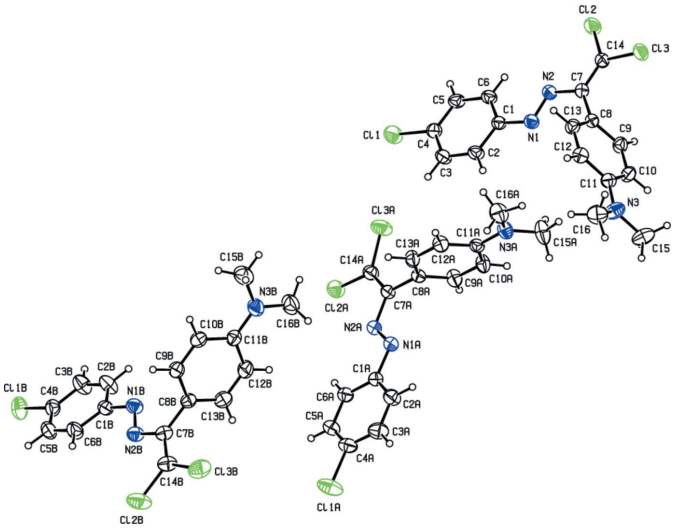

Figure 1
The molecular structures of the three molecules in the asymmetric unit of the title compound, showing the atom labelling and displacement ellipsoids drawn at the 30% probability level.

2. Structural commentary

The asymmetric unit of the title compound (Fig. 1) contains three molecules of similar shape, hereafter referred to as Mol-N1 (C1–C16/N1–N3/Cl1–Cl3), Mol-N1*A* (C1*A*–C16*A*/N1*A*–N3*A*/Cl1*A*–Cl3*A*) and Mol-N1*B* (C1*B*–C16*B*/N1*B*–N3*B*/Cl1*B*–Cl3*B*). The conformational differences between molecules Mol-N1, Mol-N1*A* and Mol-N1*B* are highlighted in an overlay diagram shown in Fig. 2. The dihedral angles between the benzene rings [C1–C6 and C8–C13 (molecule Mol-N1), C1*A*–C6*A* and C8*A*–C13*A* (molecule Mol-N1*A*), and C1*B*–C6*B* and C8*B*–C13*B* (molecule Mol-N1*B*)] of the 4-chlorophenyl and *N*,*N*-dimethylaniline groups are 69.94 (10), 79.68 (12) and 88.08 (13)°, respectively. In molecule Mol-N1, the N1—N2—C7—C14, N2—C7—C14—Cl2, N2—C7—C14—Cl3 and C8—C7—C14—Cl3 torsion angles are −178.7 (2), 3.1 (3), −176.21 (16) and 4.1 (3)°, respectively. The corresponding angles are 178.4 (2), 3.8 (3), −175.1 (2) and 2.5 (3)° for molecule Mol-N1*A*, and −175.0 (2), 0.3 (3), 179.71 (18) and −0.1 (4) for molecule Mol-N1*B*.

Table 1
Hydrogen-bond geometry (Å, °).

*Cg*1 and *Cg*4 are the centroids of the C1–C6 and C8*A*–C13*A* rings, respectively.

D—H···*A*	*D*—H	H···*A*	*D*···*A*	*D*—H···*A*
C2—H2*A*···N3*A*	0.93	2.68	3.597 (3)	167
C5*B*—H5*BA*···Cl3^{i}	0.93	2.95	3.703 (3)	139
C14—Cl3···*Cg*1^{ii}	1.71 (1)	3.55 (1)	4.083 (2)	96 (1)
C14*B*—Cl3*B*···*Cg*4^{iii}	1.71 (1)	3.85 (1)	5.300 (3)	142 (1)

Symmetry codes: (i) $x, y+1, z-1$; (ii) $-x+2, -y, -z+2$; (iii) $-x+1, -y, -z+1$.

3. Supramolecular features and Hirshfeld surface analysis

In the crystal, the molecules are connected by intermolecular C—H···N and C—H···Cl hydrogen bonds and C—Cl···π interactions, which contribute to the overall packing, forming a three-dimensional network (Table 1; Fig. 3).

Hirshfeld surface analysis was used to investigate the presence of hydrogen bonds and intermolecular interactions in the crystal structure. The Hirshfeld surfaces (Spackman & Jayatilaka, 2009) and the associated two-dimensional fingerprint plots (McKinnon *et al.*, 2007) of the title compound were calculated using *Crystal Explorer 17.5* (Turner *et al.*, 2017). The three-dimensional molecular Hirshfeld surfaces of the three molecules Mol-N1, Mol-N1*A* and Mol-N1*B* and the overall surface were generated using a high standard surface resolution colour-mapped over the normalized contact distance. The red, white and blue regions visible on the d_{norm} surfaces indicate contacts with distances shorter, longer and equal to the van der Waals radii (Fig. 4*a*). The shape-index of the Hirshfeld surface is a tool to visualize π–π stacking interactions; Fig. 4*b* clearly suggest that there are no π–π interactions in the title compound. The red spots in Fig. 4*a*

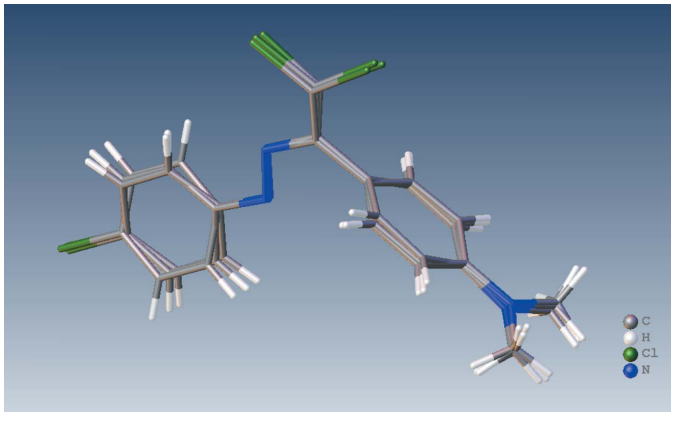

Figure 2
Overlay image of the three molecules in the asymmetric unit of the title compound.

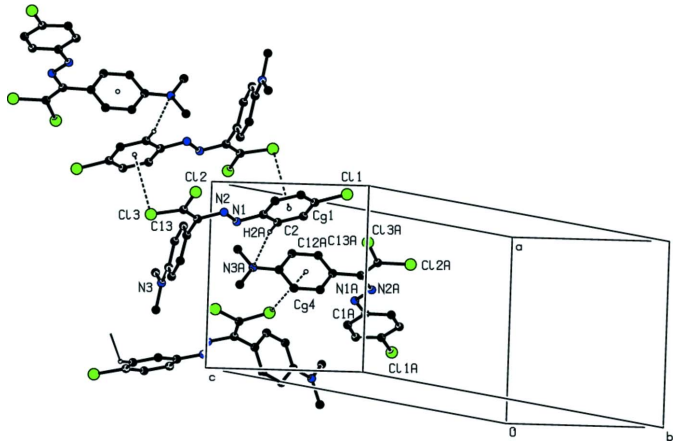

Figure 3
A partial view of the crystal packing of the title compound. Intermolecular interactions are shown as dashed lines.

Table 2
Summary of short interatomic contacts (Å) in the title compound.

Contact	Distance	Symmetry operation
(C2) H2*A*···N3*A* (C11*A*)	2.68	(*x*, *y*, *z*)
(C4) Cl1···Cl1*B* (C4*B*)	3.5403 (11)	(2 − *x*, 2 − *y*, 1 − *z*)
(C14) Cl2···Cl1 (C4)	3.6580 (11)	(2 − *x*, 1 − *y*, 2 − *z*)
(C13) H13*A*···Cl2 (C14)	3.10	(2 − *x*, −*y*, 2 − *z*)
(C14) Cl3···H5*BA* (C5*B*)	2.95	(*x*, −1 + *y*, 1 + *z*)
(C9) H9*A*···H15*D* (C15*A*)	2.60	(1 − *x*, −*y*, 2 − *z*)
(C15) H15*C*···Cl3 (C14)	3.00	(1 − *x*, −1 − *y*, 2 − *z*)
(C4) C5···H12*A* (C12)	2.95	(*x*, 1 + *y*, *z*)
(C6*A*) H6*AA*···H12*C* (C12*B*)	2.54	(*x*, *y*, *z*)
(C5*A*) H5*AA*···Cl2*A* (C14*A*)	3.10	(1 − *x*, 1 − *y*, 1 − *z*)
(C9*A*) H9*AA*···N2*B* (N1*B*)	2.92	(1 − *x*, 1 − *y*, 1 − *z*)
(C11*A*) N3*A*···H2*A* (C2)	2.68	(*x*, *y*, *z*)
(C14*A*) Cl3*A*···H16*E* (C16*A*)	3.09	(*x*, 1 + *y*, *z*)
(C14*A*) Cl3*A*···Cl1*B* (C4*B*)	3.6816 (11)	(2 − *x*, 2 − *y*, 1 − *z*)
(C4*A*) C5*A*···H15*G* (C15*B*)	2.97	(−1 + *x*, *y*, *z*)
(C3*A*) H3*AA*···H16*I* (C16*B*)	2.49	(1 − *x*, −*y*, 1 − *z*)
(C15*A*) H15*D*···H9*A* (C9)	2.60	(1 − *x*, −*y*, 2 − *z*)
(C12*A*) H12*B*···C4*B* (Cl1*B*)	2.98	(2 − *x*, 1 − *y*, 1 − *z*)
(C4*B*) Cl1*B*···Cl1 (C4)	3.5403 (11)	(2 − *x*, 2 − *y*, 1 − *z*)
(C4*B*) Cl1*B*···Cl3*A* (C14*A*)	3.6816 (11)	(2 − *x*, 2 − *y*, 1 − *z*)
(C1*B*) C4*B*···H12*B* (C12*A*)	2.98	(2 − *x*, 1 − *y*, 1 − *z*)
(C16*B*) H16*I*···H3*AA* (C3*A*)	2.49	(1 − *x*, −*y*, 1 − *z*)
(N1*B*) N2*B*···H9*AA* (C9*A*)	2.92	(1 − *x*, 1 − *y*, 1 − *z*)
(C8*B*) C9*B*···H3*BA* (C3*B*)	2.92	(*x*, −1 + *y*, *z*)
(C15*B*) H15*G*···C5*A* (C4*A*)	2.97	(1 + *x*, *y*, *z*)
(C15*B*) H15*I*···H2*BA* (C2*B*)	2.37	(2 − *x*, 1 − *y*, 1 − *z*)
(C12*B*) H12*C*···H6*AA* (C6*A*)	2.54	(*x*, *y*, *z*)
(C5*B*) H5*BA*···Cl3 (C14)	2.95	(*x*, 1 + *y*, −1 + *z*)

correspond to the relatively strong C—H···N hydrogen-bonding interactions in the crystal structure; in Mol-N1*A* it involves the N3*A* atoms of the *N*,*N*-dimethylaniline group as acceptors with the aromatic H2*A* donor atom of the chlorobenzene ring in Mol-N1 (C2—H2*A*···N3*A*).

Two-dimensional fingerprint plots are presented in Fig. 5. The red points, which represent closer contacts and negative

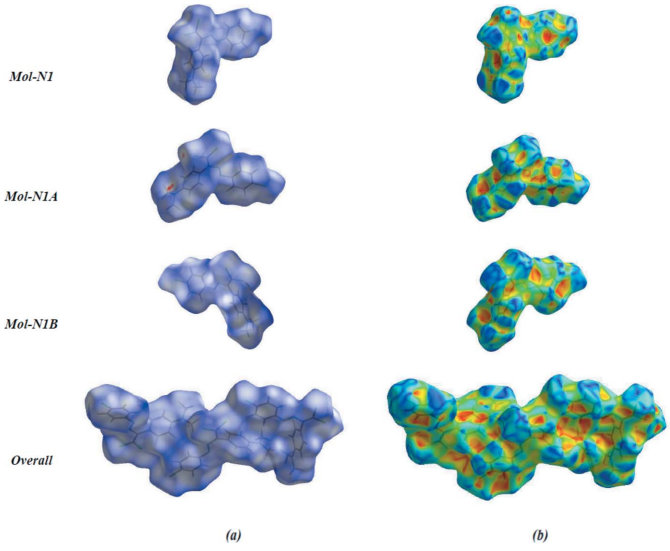

Figure 4
Hirshfeld surface of the title compound (symmetry-independent molecules Mol-N1, Mol-N1*A* and Mol-N1*B*, and overall), with (*a*) the interaction of neighbouring molecules mapped over d_{norm} and (*b*) mapped over shape-index.

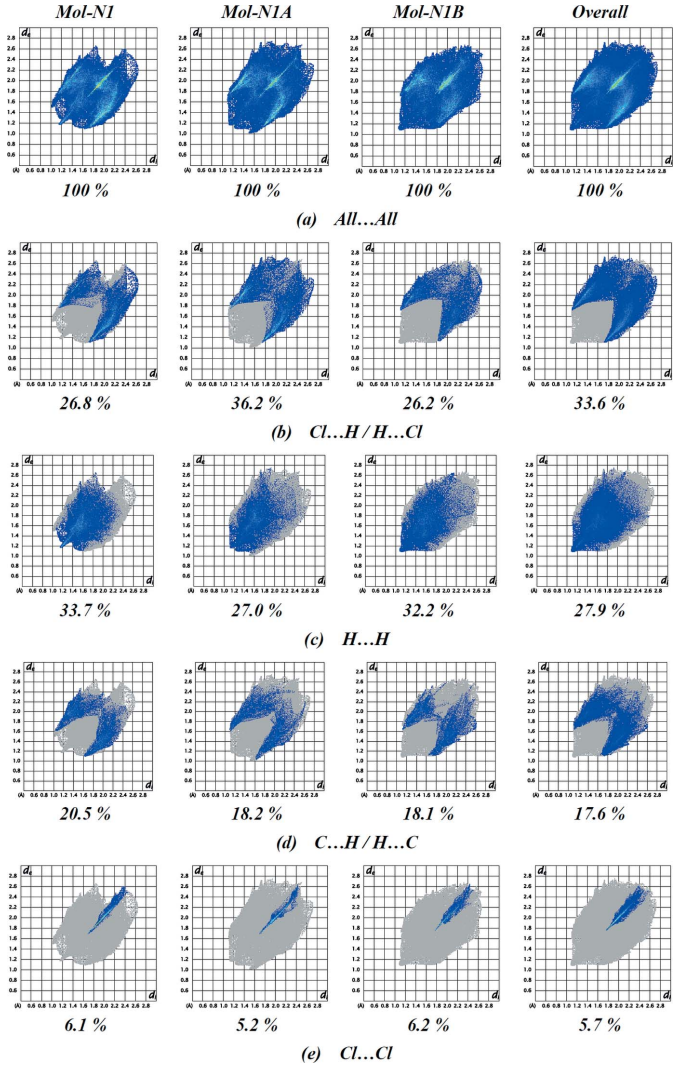

Figure 5
Fingerprint plots representative of specific interatomic contacts in the title compound (symmetry-independent molecules Mol-N1, Mol-N1*A*, Mol-N1*B* and overall), (*a*) for all interactions, and delineated into (*b*) Cl···H/H···Cl, (*c*) H···H, (*d*) C···H/H···C and (*e*) Cl···Cl interactions.

d_{norm} values on the surface, correspond to C—H···Cl interactions. The reciprocal Cl···H/H···Cl interactions appear as two symmetrical broad wings with $d_e + d_i \simeq 2.85$ Å and contribute 33.6% to the Hirshfeld surface (Fig. 5*b*). Another significant reciprocal interaction (H···H) with a contribution of 27.9% is present as broad symmetrical spikes at diagonal axes $d_e + d_i \simeq 2.2$ Å (Fig. 5*c*). The pair of characteristic wings in the fingerprint plot delineated into C···H/H···C contacts (Tables 2 and 3, Fig. 5*d*; 17.6% contribution to the Hirshfeld surface), have tips at $d_e + d_i \simeq 2.80$ Å. The Cl···Cl contacts, Fig. 5*e* (5.7% contribution), have an arrow-shaped distribution of points with the tip at $d_e = d_i = 3.50$ Å.

The other weak intermolecular interactions, *viz*. Cl···C/C···Cl (5.4%), N···H/H···N (4.7%), C···C (1.7%), Cl···N/N···Cl (1.6%), N···C/C···N (1.0%) and N···N (0.8%) contacts, show only small contributions and thus have a negligible effect on the packing.

4. Database survey

A search of the Cambridge Structural Database (CSD, Version 5.40, November 2018; Groom *et al.*, 2016) for structures having an (*E*)-1-(2,2-dichloro-1-phenylvinyl)-2-phenyldiazene skeleton gave 25 hits, of which six closely resemble the title compound, *viz*. 1-(4-bromophenyl)-2-[2,2-dichloro-1-(4-nitrophenyl)ethenyl]diazene (CSD refcode HONBOE; Akkurt *et al.*, 2019), 1-(4-chlorophenyl)-2-[2,2-dichloro-1-(4-nitrophenyl)ethenyl]diazene (HONBUK; Akkurt *et al.*, 2019), 1-(4-chlorophenyl)-2-[2,2-dichloro-1-(4-fluorophenyl)ethenyl]diazene (HODQAV; Shixaliyev *et al.*, 2019), 1-[2,2-dichloro-1-(4-nitrophenyl)ethenyl]-2-(4-fluorophenyl)diazene (XIZREG; Atioğlu *et al.*, 2019), 1,1-[methylenebis(4,1-phenylene)]bis[(2,2-dichloro-1-(4-nitrophenyl)ethenyl]diazene (LEQXIR; Shixaliyev *et al.*, 2018), 1,1-[methylenebis(4,1-phenylene)]bis{[2,2-dichloro-1-(4-chlorophenyl) ethenyl]-diazene} (LEQXOX; Shixaliyev *et al.*, 2018).

In the crystal structures of HONBOE and HONBUK, the aromatic rings form dihedral angles of 60.9 (2) and 64.1 (2)°, respectively. Molecules are linked through weak *X*···Cl contacts [*X* = Br for HONBOE, and Cl for HONBUK], C—H···Cl and C—Cl···π interactions into sheets parallel to (001). Additional van der Waals interactions consolidate the three-dimensional packing. In the crystal of HODQAV, molecules are stacked in columns along [100] *via* weak C—H···Cl hydrogen bonds and face-to-face π–π stacking interactions. The crystal packing is further stabilized by short Cl···Cl contacts. In XIZREG, molecules are linked by C—H···O hydrogen bonds into zigzag chains running along [001]. The crystal packing is further stabilized by C—Cl···π, C—F···π and N—O···π interactions. In the crystal of LEQXIR, C—H···N and C—H···O hydrogen bonds and Cl···O contacts were found, and in LEQXOX, C—H···N and Cl···Cl contacts are observed.

5. Synthesis and crystallization

The title compound was synthesized according to a reported literature protocol (Maharramov *et al.*, 2018). A 20 ml screw-neck vial was charged with DMSO (10 ml), (*E*)-4-[(2-(4-chlorophenyl)hydrazineylidene]methyl)-*N*,*N*-dimethylaniline (274 mg, 1 mmol), tetramethylethylenediamine (TMEDA) (295 mg, 2.5 mmol), CuCl (2 mg, 0.02 mmol) and CCl_4 (20 mmol, 10 equiv). After 1–3 h (until TLC analysis showed complete consumption of the corresponding Schiff base), the reaction mixture was poured into a ∼0.01 *M* solution of HCl (100 mL, pH = ∼2–3) and extracted with dichloromethane (3 × 20 ml). The combined organic phase was washed with water (3 x 50 ml), brine (30 ml), dried over anhydrous Na_2SO_4 and concentrated *in vacuo* in a rotary evaporator. The residue was purified by column chromatography on silica gel using appropriate mixtures of hexane and dichloromethane (3/1–1/1) to give an orange solid. Yield: 72%; mp 408 K. Analysis: calculated for $C_{16}H_{14}Cl_3N_3$: C 54.19, H 3.98, N 11.85; found: C 54.08, H 3.91, N 11.82%. ^{1}H NMR (300 MHz, $CDCl_3$) δ 3.05 (6H, NMe_2), 6.79–7.79 (8H, Ar). ^{13}C NMR (75 MHz, $CDCl_3$) δ 152.41, 151.45, 150.29, 137.26, 135.11, 131.08, 129.27, 124.50, 119.11, 111.48, 40.29. ESI–MS: *m*/*z*: 355.48 $[M + H]^+$.

Crystals suitable for X-ray analysis were obtained by slow evaporation of an ethanol solution.

Table 3
Experimental details.

Crystal data	
Chemical formula	$C_{16}H_{14}Cl_3N_3$
M_r	354.65
Crystal system, space group	Triclinic, $P\overline{1}$
Temperature (K)	296
a, *b*, *c* (Å)	9.7515 (5), 9.8203 (5), 26.6696 (16)
α, β, γ (°)	92.338 (2), 91.212 (2), 94.048 (2)
V (Å^3)	2544.7 (2)
Z	6
Radiation type	Mo *K*α
μ (mm^{-1})	0.54
Crystal size (mm)	0.24 × 0.15 × 0.09
Data collection	
Diffractometer	Bruker APEXII PHOTON 100 detector
Absorption correction	Multi-scan (*SADABS*; Krause *et al.*, 2015)
T_{min}, T_{max}	0.894, 0.946
No. of measured, independent and observed [$I > 2\sigma(I)$] reflections	40829, 9634, 6689
R_{int}	0.056
(sin $\theta/\lambda)_{max}$ (Å^{-1})	0.610
Refinement	
$R[F^2 > 2\sigma(F^2)]$, $wR(F^2)$, *S*	0.041, 0.115, 1.01
No. of reflections	9634
No. of parameters	601
H-atom treatment	H-atom parameters constrained
$\Delta\rho_{max}$, $\Delta\rho_{min}$ (e Å^{-3})	0.29, −0.30

Computer programs: *APEX3* and *SAINT* (Bruker, 2007), *SHELXT* (Sheldrick, 2015*a*), *SHELXL* (Sheldrick, 2015*b*), *ORTEP-3 for Windows* (Farrugia, 2012), *OLEX2* (Dolomanov *et al.*, 2009), *PLATON* (Spek, 2020) and *publCIF* (Westrip, 2010).

6. Refinement

Crystal data, data collection and structure refinement details are summarized in Table 3. All C-bound H atoms were refined using a riding model with *d*(C—H) = 0.93 Å, U_{iso}(H) = 1.2U_{eq}(C) for aromatic H atoms, and 0.96 Å, U_{iso}(H) = 1.5U_{eq}(C) for methyl H atoms. Owing to poor agreement between observed and calculated intensities, five outliers ($\overline{11}$ 0 4), (4 $\overline{10}$ 13), ($\overline{5}$ 8 8), ($\overline{7}$ 2 18) and (1 8 14) were omitted in the final cycles of refinement.

Funding information

This work was funded by the Science Development Foundation under the President of the Republic of Azerbaijan [grant No. EIF/MQM/Elm-Tehsil-1–2016-1(26)–71/06/4].

References

Afkhami, F. A., Mahmoudi, G., Gurbanov, A. V., Zubkov, F. I., Qu, F., Gupta, A. & Safin, D. A. (2017). *Dalton Trans.* **46**, 14888–14896.
Akkurt, M., Shikhaliyev, N. Q., Suleymanova, G. T., Babayeva, G. V., Mammadova, G. Z., Niyazova, A. A., Shikhaliyeva, I. M. & Toze, F. A. A. (2019). *Acta Cryst.* E**75**, 1199–1204.

Asadov, Z. H., Rahimov, R. A., Ahmadova, G. A., Mammadova, K. A. & Gurbanov, A. V. (2016). *J. Surfactants Deterg.* **19**, 145–153.
Atioğlu, Z., Akkurt, M., Shikhaliyev, N. Q., Suleymanova, G. T., Bagirova, K. N. & Toze, F. A. A. (2019). *Acta Cryst.* E**75**, 237–241.
Bruker (2007). *APEX2* and *SAINT*. Bruker AXS Inc., Madison, Wisconsin, USA.
Dolomanov, O. V., Bourhis, L. J., Gildea, R. J., Howard, J. A. K. & Puschmann, H. (2009). *J. Appl. Cryst.* **42**, 339–341.
Farrugia, L. J. (2012). *J. Appl. Cryst.* **45**, 849–854.
Groom, C. R., Bruno, I. J., Lightfoot, M. P. & Ward, S. C. (2016). *Acta Cryst.* B**72**, 171–179.
Gurbanov, A. V., Maharramov, A. M., Zubkov, F. I., Saifutdinov, A. M. & Guseinov, F. I. (2018). *Aust. J. Chem.* **71**, 190–194.
Krause, L., Herbst-Irmer, R., Sheldrick, G. M. & Stalke, D. (2015). *J. Appl. Cryst.* **48**, 3–10.
Maharramov, A. M., Shikhaliyev, N. Q., Suleymanova, G. T., Gurbanov, A. V., Babayeva, G. V., Mammadova, G. Z., Zubkov, F. I., Nenajdenko, V. G., Mahmudov, K. T. & Pombeiro, A. J. L. (2018). *Dyes Pigments*, **159**, 135–141.
Mahmudov, K. T., Gurbanov, A. V., Guseinov, F. I. & Guedes da Silva, M. F. C. (2019). *Coord. Chem. Rev.* **387**, 32–46.
Mahmudov, K. T. & Pombeiro, A. J. L. (2016). *Chem. Eur. J.* **22**, 16356–16398.
McKinnon, J. J., Jayatilaka, D. & Spackman, M. A. (2007). *Chem. Commun.* pp. 3814–3816.
Sheldrick, G. M. (2015*a*). *Acta Cryst.* A**71**, 3–8.
Sheldrick, G. M. (2015*b*). *Acta Cryst.* C**71**, 3–8.
Shikhaliyev, N. Q., Ahmadova, N. E., Gurbanov, A. V., Maharramov, A. M., Mammadova, G. Z., Nenajdenko, V. G., Zubkov, F. I., Mahmudov, K. T. & Pombeiro, A. J. L. (2018). *Dyes Pigments*, **150**, 377–381.
Shikhaliyev, N. Q., Çelikesir, S. T., Akkurt, M., Bagirova, K. N., Suleymanova, G. T. & Toze, F. A. A. (2019). *Acta Cryst.* E**75**, 465–469.
Spackman, M. A. & Jayatilaka, D. (2009). *CrystEngComm*, **11**, 19–32.
Spek, A. L. (2020). *Acta Cryst.* E**76**, 1–11.
Turner, M. J., McKinnon, J. J., Wolff, S. K., Grimwood, D. J., Spackman, P. R., Jayatilaka, D. & Spackman, M. A. (2017). CrystalExplorer17. The University of Western Australia.
Westrip, S. P. (2010). *J. Appl. Cryst.* **43**, 920–925.